The EMBO Journal (2012) 31, 606–615 | © 2012 European Molecular Biology Organization | All Rights Reserved 0261-4189/12
www.embojournal.org

THE EMBO JOURNAL

Transcription and histone methylation changes correlate with imprint acquisition in male germ cells

Amandine Henckel[1], Karim Chebli, Satya K Kota, Philippe Arnaud[2,3,*] and Robert Feil[3,*]

Institute of Molecular Genetics (IGMM), CNRS, Universities of Montpellier I and II, Montpellier, France

Genomic imprinting in mammals is controlled by DNA methylation imprints that are acquired in the gametes, at essential sequence elements called 'imprinting control regions' (ICRs). What signals paternal imprint acquisition in male germ cells remains unknown. To address this question, we explored histone methylation at ICRs in mouse primordial germ cells (PGCs). By 13.5 days *post coitum* (d.p.c.), H3 lysine-9 and H4 lysine-20 trimethylation are depleted from ICRs in male (and female) PGCs, indicating that these modifications do not signal subsequent imprint acquisition, which initiates at ~15.5 d.p.c. Furthermore, during male PGC development, H3 lysine-4 trimethylation becomes biallelically enriched at 'maternal' ICRs, which are protected against DNA methylation, and whose promoters are active in the male germ cells. Remarkably, high transcriptional read-through is detected at the paternal ICRs *H19*-DMR and Ig-DMR at the time of imprint establishment, from one of the strands predominantly. Combined, our data evoke a model in which differential histone modification states linked to transcriptional events may signal the specificity of imprint acquisition during spermatogenesis.

The EMBO Journal (2012) **31,** 606–615. doi:10.1038/emboj.2011.425; Published online 25 November 2011
Subject Categories: chromatin & transcription; development
Keywords: DNA methylation; epigenetic; genomic imprinting; histone methylation; primordial germ cells

Introduction

Mammalian imprinted genes are organised in clusters and their parental allele-specific expression is regulated by essential, CpG-rich, sequence elements called 'imprinting control regions' (ICRs; Bartolomei, 2009; Arnaud, 2010). It is not known why some ICRs acquire DNA methylation imprints in the female germ line, while others become methylated specifically in the male germ line. However, in both the germ lines *de-novo* DNA methyltransferase DNMT3A is involved in imprint acquisition (Kaneda *et al*, 2004; Kato *et al*, 2007). The related DNMT3L protein can form complexes with DNMT3A and plays an essential role in imprint acquisition as well (Bourc'his *et al*, 2001; Hata *et al*, 2002; Kato *et al*, 2007). Interestingly, DNMT3L can bind to histone H3 *in vitro*, but H3 lysine-4 dimethylation, and in particular H3-K4 trimethylation (H3K4me3), was found to prevent its association with chromatin (Ooi *et al*, 2007). Recent studies show that DNMT3A itself is also sensitive to the H3 lysine-4 methylation status. Its 'ATRX-DNMT3-DNMTL' (ADD) domain binds to the H3 tail most efficiently when lysine-4 is unmethylated (Otani *et al*, 2009; Zhang *et al*, 2010; Li *et al*, 2011). Despite a suspected involvement of histone methylation states in the recruitment of DNA methyltransferase complexes, so far no studies have directly assessed chromatin at imprinted loci in germ cells to test this hypothesis.

Many ICRs acquire their DNA methylation in the female germ line (Arnaud, 2010). Two well-known 'maternal ICRs' are the CpG island/promoter of the *Snrpn* gene (Shemer *et al*, 1997), which controls the Prader–Willi Syndrome imprinted domain on central chromosome 7, and the KvDMR1, a CpG island/promoter that controls the *Kcnq1* domain on distal chromosome 7 (Fitzpatrick *et al*, 2002). Only four differentially methylated regions (DMRs) are known to acquire their methylation during spermatogenesis, a pre-meiotic process that initiates during fetal stages of development (Arnaud, 2010). The best-characterised 'paternal ICRs' are the *H19* DMR controlling the *Igf2-H19* domain on mouse distal chromosome 7 (Tremblay *et al*, 1995) and the Ig-DMR, which controls the *Dlk1-Dio3* domain on mouse distal chromosome-12 (Lin *et al*, 2003).

Maternal ICRs comprise gene promoters, whereas paternal ICRs are intergenic non-promoter regions. This intriguing distinction might somehow contribute to the specificity of imprint acquisition. For instance, specific histone modifications such as H3K4me3 are linked to promoter activity, at least in somatic cells (Mikkelsen *et al* 2007; Zhao *et al*, 2007), and could prevent acquisition of *de-novo* DNA methylation (Ooi *et al*, 2007; Ciccone *et al*, 2009; Zhang *et al*, 2010). Here, we explore histone methylation in mouse primordial germ cells (PGCs), and in later-stage germ cells, with particular emphasis on the male germ line. A carrier chromatin immunoprecipitation (cChIP) approach was developed, adapted to small batches of FACS-sorted cells, to assess ICRs at critical stages of spermatogenesis. A main finding is that at maternal ICRs protection against DNA methylation in male germ cells correlates with promoter activity and biallelic enrichment of H3 lysine-4 (tri)methylation. At the paternal ICRs *H19*-DMR and Ig-DMR, in contrast, chromatin is organised differently and here acquisition of DNA methylation correlates with transcriptional read-through. Our data evoke a putative link

*Corresponding authors. P Arnaud, GreD, CNRS, UMR6247, Clermont Université, INSERM U931, 28 Place Henri Dunant, BP38, 63001 Clermont-Ferrand, France. Tel.: +33 473178380; Fax: +33 473276132; E-mail: philippe.arnaud@u-clermont1.fr or R Feil, Institute of Molecular Genetics (IGMM), CNRS, UMR5535, Universities of Montpellier I and II, 1919 Route de Mende, 34293 Montpellier, France. Tel.: +33 43 435 9663; Fax: +33 43 435 9634; E-mail: robert.feil@igmm.cnrs.fr
[1]Present address: Max Planck Institute of Immunobiology and Epigenetics, Freiburg, Germany
[2]Present address: GreD, CNRS, UMR6247, Clermont Université, INSERM U931, Clermont-Ferrand, France
[3]Co-senior authors

Received: 28 June 2011; accepted: 24 October 2011; published online: 25 November 2011

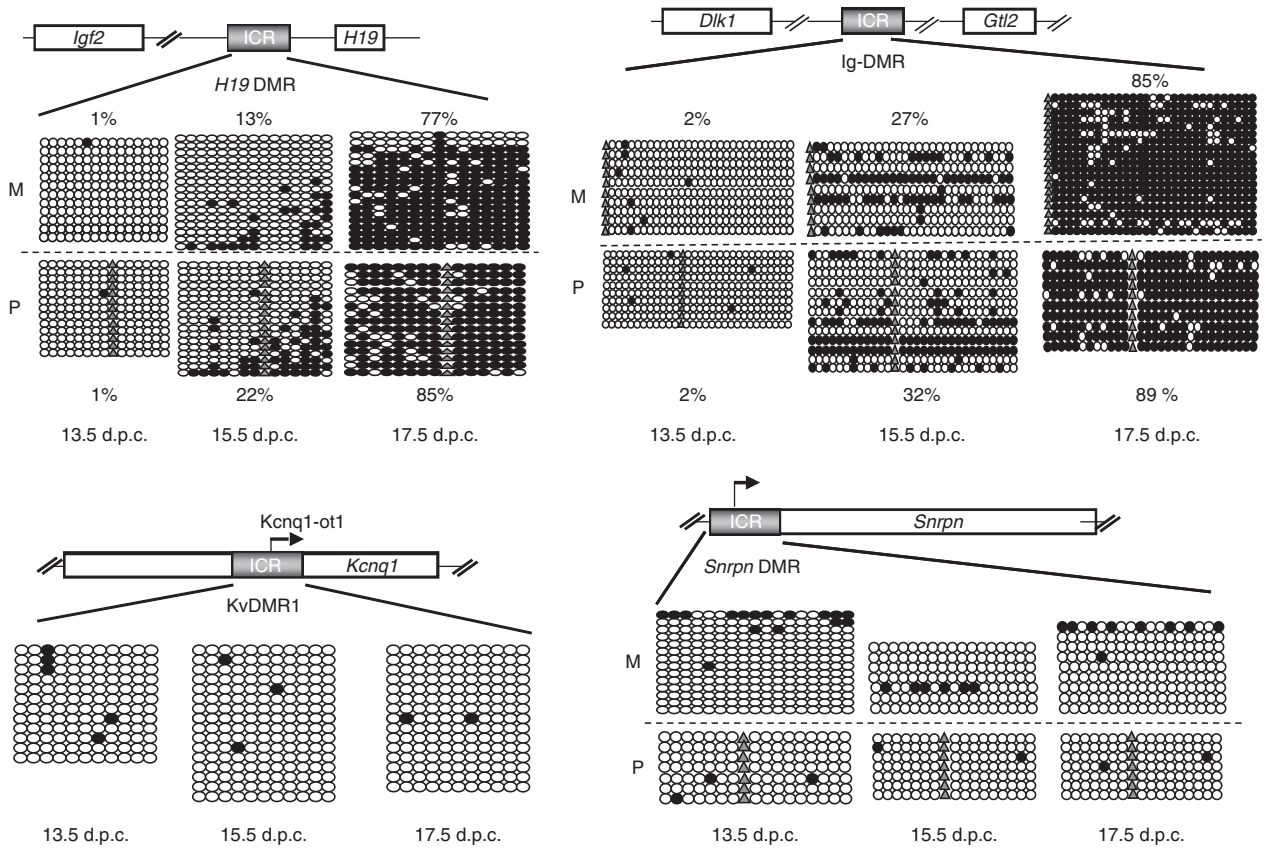

Figure 1 Dynamics of ICR methylation in male germ cells. Analysed ICRs (grey boxes) and genes (empty boxes) are represented. Representative data from one experiment are shown for each of the regions analysed. Each horizontal row of circles represents the CpG dinucleotides on an individual chromosome. Solid circles depict methylated CpGs, open circles unmethylated CpGs. Parental origin (M, maternal; P, paternal) was determined using SNPs. Grey triangles show CpGs that are absent due to SNPs. For the *H19* DMR and Ig-DMR, the measured percentile level of methylation (% methylated CpGs/total CpGs analysed) is indicated for the maternal and the paternal alleles. These levels were reproduced in independently repeated experiments.

between transcription, histone methylation, and imprint acquisition during spermatogenesis.

Results

Dynamics of DNA methylation acquisition in male germ cells

Embryos were derived that were intra-specific hybrid between C57BL/6J and *M. m. molossinus* strain JF1 (Koide *et al*, 1998) and transgenic for a GFP gene driven by *Oct4* regulatory sequences (Yoshimizu *et al*, 1999). Gonads were dissected at fetal stages. Batches of FACS-sorted germ cells were obtained for DNA methylation, transcription, and chromatin studies. Single-nucleotide polymorphisms (SNPs) between C57BL/6J and JF1 allowed us to distinguish the parental chromosomes (Henckel *et al*, 2009). First, we determined by bisulphite sequencing the timing of DNA methylation acquisition in germ cells of male fetuses. At four ICRs analysed, no DNA methylation was detected at 13.5 d.p.c., confirming that complete DNA demethylation had occurred at this stage (Figure 1). At the *H19* DMR, initial acquisition of methylation was observed at 15.5 d.p.c., and by 17.5 d.p.c., DNA methylation was almost complete. Less pronouncedly than in some studies (Davis *et al*, 2000), but comparable to others (Kato *et al*, 2007; Lee *et al*, 2010), imprint acquisition was delayed on the maternal compared with the paternal allele. At the Ig-DMR controlling the *Dlk1-Dio3* domain (Lin *et al*, 2003), the timing of imprint acquisition was comparable to the *H19* DMR, with partial acquisition at 15.5 d.p.c. and almost full DNA methylation at 17.5 d.p.c. The measured levels of DNA methylation were not much different on the parental chromosomes at 15.5 d.p.c. Also at the DMR of the *Gpr1-Zdbf2* imprinted domain on mouse chromosome 1 (Hiura *et al*, 2010), some CpG dinucleotides had acquired methylation by 15.5 d.p.c, and almost all CpGs were fully methylated at 17.5 d.p.c. (Supplementary Figure S1). The maternal ICRs KvDMR1 and *Snrpn* DMR, as expected, remained unmethylated in the male germ cells at the stages analysed (Figure 1).

cChIP adapted to small numbers of FACS-sorted cells

To explore histone methylation in small batches of PGCs, we adapted a cChIP approach (O'Neill *et al*, 2006). Small batches of FACS-sorted mouse cells were mixed with an excess of *Drosophila melanogaster* S2 cells, nuclei were purified, followed by partial MNase digestion, purification of chromatin fragments of 1–7 nucleosomes in length, and immunoprecipitation (Figure 2A). First, we checked whether our methodology faithfully revealed the allele specificity of H3 and H4 methylation at ICRs in the negatively sorted (GFP minus) somatic cells. Indeed, using ~75 000 somatic cells per cChIP, we obtained allelic precipitation at the KvDMR1 (Figure 2B),

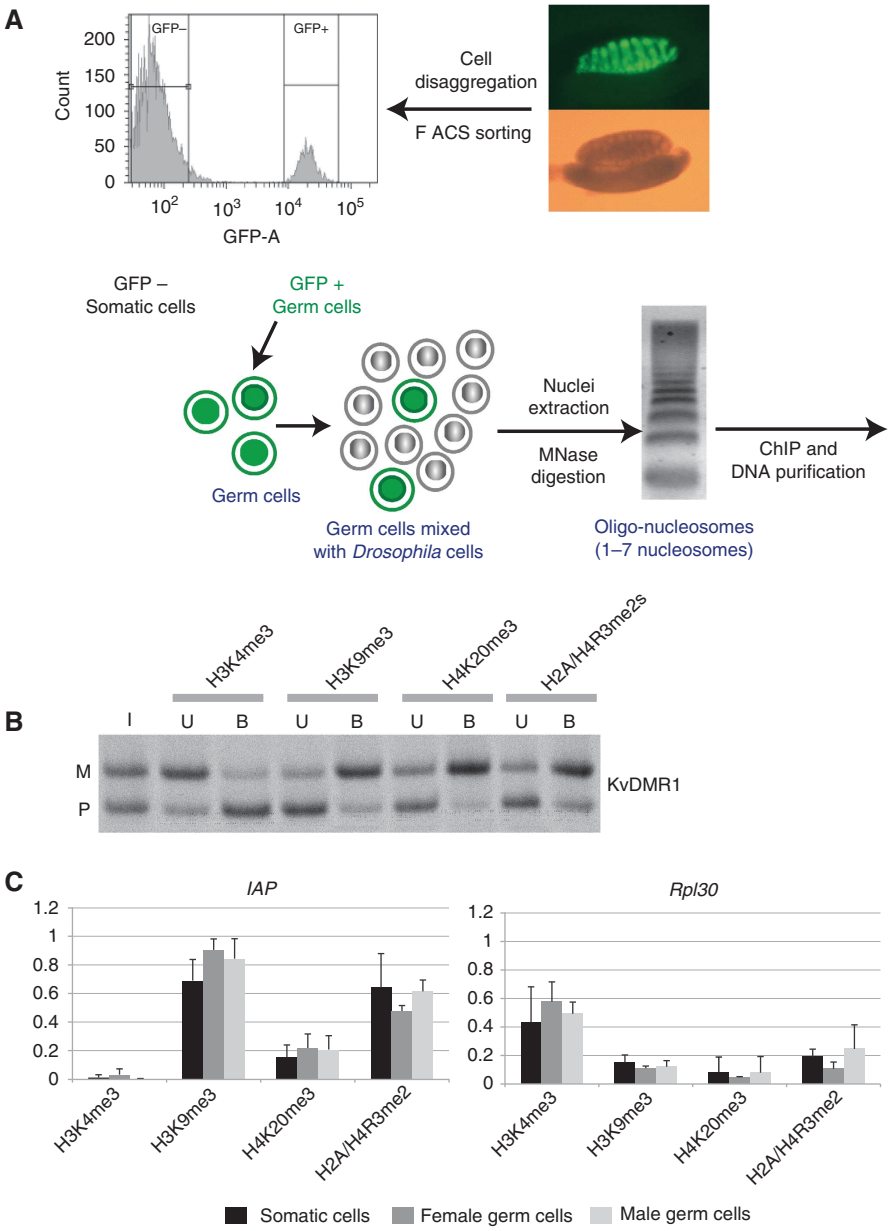

Figure 2 Overview and validation of a carrier ChIP approach. (**A**) Schematic overview. PGCs were obtained from embryos that were *Oct4*-GFP transgenic. In the 13.5 d.p.c. male gonad shown, green fluorescence visualises the PGCs. (**B**) PCR-SSCP analysis after cChIP on somatic control cells with antisera directed against H3K4me3, H3K9me3, H4K20me3, and H2A/H4R3me2s. Results on the KvDMR1 are shown, for input chromatin (I) and antibody-bound (B), and -unbound (U) fractions. In this qualitative assay, the PCR amplifications were close to saturation. (**C**) Precipitation of H3K4me3, H3K9me3, H4K20me3, and H2A/H4R3me2s in 13.5 d.p.c. female germ cells (grey), male germ cells (white), and somatic control cells (black) at *Rpl30* and IAP elements. cChIP was performed, at least, in triplicate. Bound chromatin fractions were quantified by real-time PCR and corrected for background precipitation (percentile precipitation with standard deviation).

and at *Snrpn* DMR, *H19* DMR, and the Ig-DMR (Supplementary Figure S2). As in earlier studies on somatic cells (Delaval *et al*, 2007; Verona *et al*, 2008; Pannetier *et al*, 2008; Henckel *et al*, 2009), H3K9me3 and H4K20me3 were enriched on the DNA-methylated allele, and H3K4me3 on the unmethylated allele. Using smaller batches of FACS-sorted somatic cells, the prepared input chromatin was often biased towards one of the parental alleles, and quantification of the precipitated chromatin was not reproducible between experiments. For our subsequent chromatin studies on 13.5 and 15.5 d.p.c germ cells, therefore, we decided to use 75 000–100 000 cells per cChIP. cChIP could not be performed at 17.5 d.p.c., given the relative difficulty in trypsinising and sorting gonadal cells at this developmentally advanced stage.

Reprogramming of histone methylation at ICRs during PGC development

Since in 13.5 d.p.c. germ cells there was no detectable DNA methylation at ICRs, we asked whether associated histone methylations had been lost as well. Locus-specific precipitation levels of repressive histone modifications (H3K9me3, H4K20me3, and H2A/H4R3me2s) were normalised against precipitation at intra-cisternal-A particle (IAP) sequences. These repeat elements exceptionally remain DNA methylated

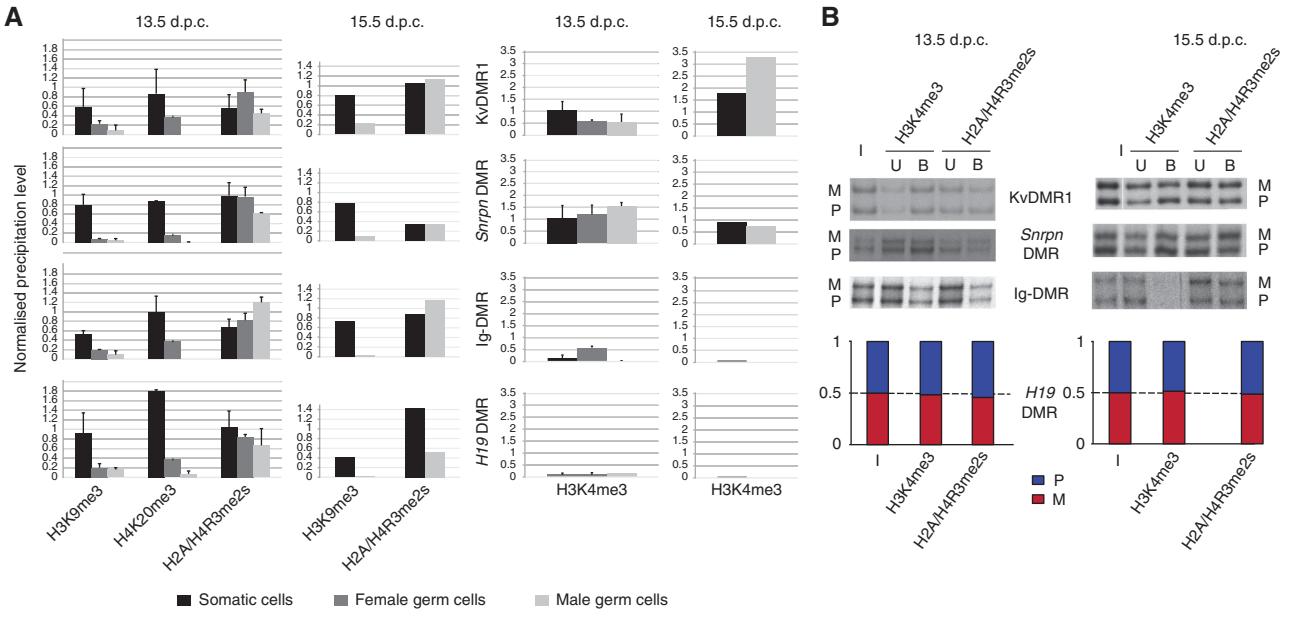

Figure 3 Reprogramming of histone methylation at ICRs in PGCs. (**A**) To the left, quantification of H3K9me3, H4K20me3, and H2A/H4R3me2s in male (white) and female (grey) PGCs and somatic control cells (black; a mixture of male and female cells). Relative enrichment is defined as the ratio between the bound (with subtracted background) and the input chromatin, and was normalised to the (bound-background)/input ratio obtained for IAP elements. To the right, quantification of H3K4me3. Relative enrichment was calculated as the ratio between the bound fraction (with subtracted background) and input and was normalised to the (bound-background)/input ratio obtained for *Rpl30*. Experiments were performed at least in triplicate. Standard deviations are not given for experiments at 15.5 d.p.c., which were performed twice on male PGCs. Female PGCs were not analysed by ChIP at 15.5 d.p.c. (**B**) PCR-SSCP analysis (KvDMR1, *Snrpn* DMR, Ig-DMR) or real-time PCR-based allelic discrimination (*H19* DMR) after cChIP on male germ cells. At all four ICRs analysed, the histone methylations studied were similarly precipitated from the maternal (M) and the paternal (P) alleles (the ratio between the parental alleles were in all cases smaller than 1.5). In this qualitative assay, the PCR amplifications were close to saturation.

in developing PGCs despite the global DNA demethylation (Lane *et al*, 2003). Concordantly, H3K9me3, H4K20me3, and H2A/H4R3me2s at IAP elements were similarly high in the 13.5 d.p.c. PGCs as in somatic cells (Figure 2C). At all ICRs analysed, in contrast, the male 13.5 d.p.c. PGCs showed almost complete absence of H3K9me3 and H4K20me3 (Figure 3A). Similarly, at 15.5 d.p.c. we found H3K9me3 to be absent from ICRs in male germ cells. Also in female PGCs, we detected strongly reduced H3K9me3 and H4K20me3 at all four ICRs analysed (Figure 3A). Thus, together with the loss of DNA methylation, the associated H3K9me3 and H4K20me3 had been lost in the developing male and female PGCs as well.

In somatic cells, symmetrical dimethylation on arginine-3 of histones H2A and H4 (H2A/H4R3me2s) is enriched on the DNA-methylated allele of ICRs as well (Verona *et al*, 2008; Henckel *et al*, 2009; Supplementary Figure S2). Interestingly, despite the lack of DNA methylation, H2A/H4R3me2s was still present at high levels at all four ICRs analysed in the PGCs (male and female), at 13.5 and 15.5 d.p.c. (Figure 3A). By conventional PCR, followed by electrophoretic discrimination of Single-Strand Conformation Polymorphisms (SSCPs), it was found to be present on both the parental chromosomes at all four ICRs analysed (Figure 3B).

Acquisition of biallelic H3 lysine-4 methylation correlates with protection against DNA methylation

Next, we explored whether H3 lysine-4 methylation could be enriched at maternal ICRs in male germ cells. As an internal control, we chose a housekeeping gene, *Rpl30* (Ribosomal protein L30), which is expressed at high levels in both male and female germ cells (Supplementary Figure S3). We focused on H3 lysine-4 trimethylation (H3K4me3) given its direct link with active promoters in somatic cells (Bernstein *et al*, 2006; Zhao *et al*, 2007). Indeed, in the PGCs this modification showed high levels of precipitation at *Rpl30*, as in somatic cells (Figure 2C). In the male PGCs, high levels of H3K4me3 were detected at the maternal ICRs *Snrpn* DMR and KvDMR1, at both 13.5 and 15.5 d.p.c. (Figure 3A). H3K4me3 was equally present on both the parental chromosomes (Figure 3B).

If H3 lysine-4 methylation prevents acquisition of DNA methylation *in vivo*, one expects this modification to be absent from paternal ICRs at the time of imprint acquisition in the male germ cells. This is precisely what we found at Ig-DMR and *H19* DMR, at 13.5 d.p.c., and even more pronouncedly so at 15.5 d.p.c. (Figure 3A), when paternal DNA methylation establishment initiates (Figure 1).

Transcription is linked to the specificity of imprint acquisition

Next, we explored whether the differential histone methylation between ICRs could be linked to transcriptional events. cDNAs were synthesised from total RNAs using random oligonucleotides, followed by quantitative PCR amplification (Supplementary Table S1). First, we analysed the maternal ICRs *Snrpn* DMR and KvDMR1. Both these CpG island promoters produce mono-allelic, long transcripts in somatic cells, which are readily detected downstream of their

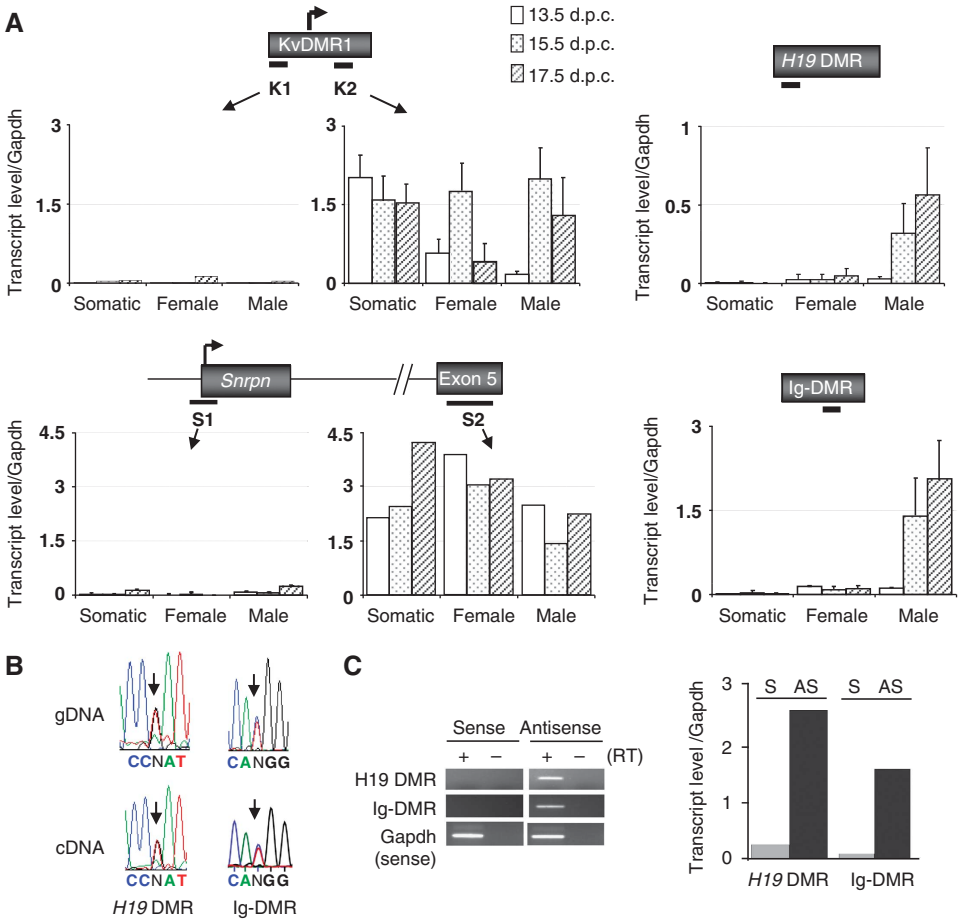

Figure 4 Biallelic transcription across paternal ICRs at the time of imprint establishment. (**A**) Quantitative RT–PCR analysis of male and female germ cells and gonad somatic control cells (somatic) at 13.5, 15.5, and 17.5 d.p.c. Black dashes indicate the positions of the amplified regions (see Supplementary Table SI). The *H19* DMR and Ig-DMR were each analysed by quantitative PCR at one other region as well, which gave comparable results (Figure 5; Supplementary Figure S6). For KvDMR1 and *Snrpn* DMR, amplifications were performed upstream (K1 and S1, respectively) and downstream (K2 and S2, respectively) of the known transcription start site (see also Supplementary Figure S4). Measured levels of transcripts for each of the analysed regions are normalised to that of *Gapdh*. (**B**) *H19* DMR and Ig-DMR germ cell transcripts are biallelic. Sequence traces of RT–PCR products are shown in the lower panel (cDNA), with an arrow indicating SNPs. As control sequences, sequence traces obtained from genomic DNA (gDNA) are shown. (**C**) Strand-specific RT–PCR analysis. Reverse transcription reactions with 15.5 d.p.c male PGC RNA were performed with primers specific for the sense (S) or antisense (AS) *H19*-DMR and Ig-DMR transcripts, respectively. As a positive control, reactions were multiplexed with a primer set specific for *Gapdh*, further used to normalise the data. Non-quantitative (left panel) and quantitative (right panel) analyses are shown.

transcriptional initiation sites (Bartolomei, 2009). With a primer pair at the 3′ side of the KvDMR1, high levels of transcript were detected in both male and female PGCs, at 13.5, 15.5 and 17.5 d.p.c. (Figure 4A). To assess whether transcription originated from within the KvDMR1, we also amplified the cDNA with a primer pair at the 5′ extremity of the KvDMR1, upstream of the somatic transcription start site. As in somatic cells, no amplification was detected in the germ cells at this region. At the *Snrpn* DMR, transcripts are readily amplified (from both the parental alleles) between *Snrpn* exons 1 and 3 (Supplementary Figure S4); similarly, high transcript levels were detected with primers at exon 5 (Figure 4A). A second primer pair, located directly 5′ of its somatic promoter (see Figure 4A), and primers spanning further upstream U1 promoters (Supplementary Figure S4), did not give significant amplification. Although we did not determine the precise transcription start sites, these results suggest that the KvDMR1 and Snrpn DMR act as promoters in PGCs as well. At several other maternal ICRs analysed (*ZacI, Grb10, Impact*), we also detected promoter activity in the male germ cells at 15.5 and 17.5 d.p.c. (Supplementary Figure S4).

Next, we explored transcription at the *H19* DMR and the Ig-DMR (Figure 4A). In agreement with earlier reports (Drewell *et al*, 2002; Schoenfelder *et al*, 2007), only low levels of transcription were detected at the *H19* DMR in somatic tissues and embryos (Supplementary Figure S5). Hardly any transcription was detected at the *H19* DMR and the Ig-DMR in the FACS-sorted somatic control cells either. In female PGCs, only weak transcription was observed at the two paternal ICRs at the three developmental stages analysed (Figure 4A; Supplementary Figure S5).

A strikingly different picture emerged analysing male germ cells. Whereas at 13.5 d.p.c., virtually no transcription is detected at the Ig-DMR and *H19* DMR, the signal increased tremendously by 15.5 d.p.c., at the onset of imprint acquisition, to levels comparable to those of the housekeeping genes *Gapdh* and *Rpl30*. The high expression of Ig-DMR and

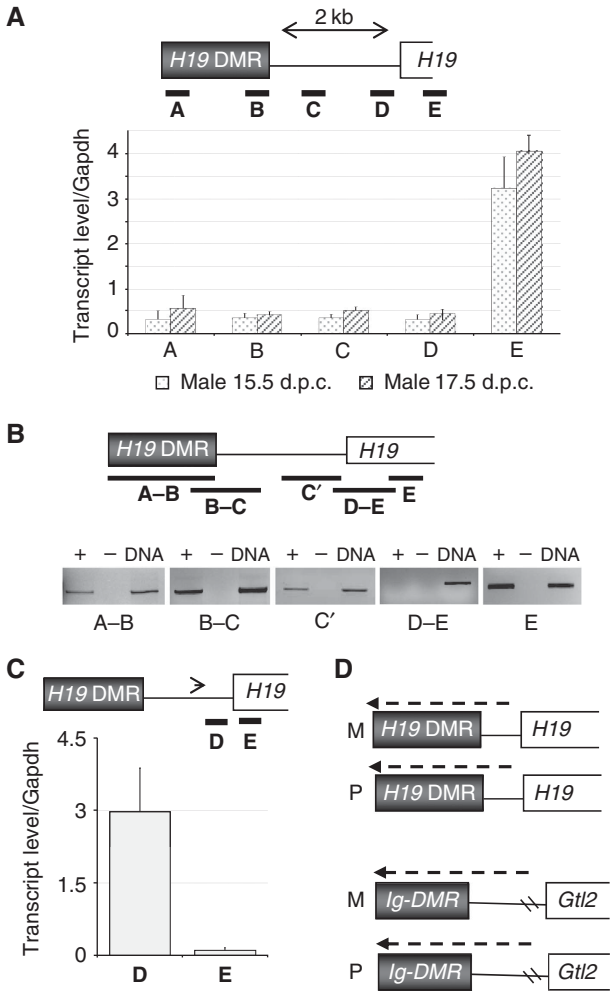

Figure 5 Characterisation of *H19* DMR and Ig-DMR non-coding RNAs in male germ cells. (**A**) Quantitative RT–PCR analysis at 15.5 and 17.5 d.p.c. Five regions (regions A–E, black bars) were analysed and measured transcript levels were normalised to that of *Gapdh*. (**B**) RT–PCR in male PGCs at 15.5 d.p.c. (followed by gel electrophoresis). Five regions (A–B, B–C, C′, D–E, E; black bars) were analysed. Region D–E, spanning the *H19* promoter, failed to amplify in multiple experiments. +, With reverse transcriptase (RT); −, without RT; DNA, control amplification on genomic DNA. (**C**) Quantification following strand-specific RT–PCR. The arrowhead indicates the relative position of the strand-specific oligonucleotide used to produce cDNA. Measured levels of transcripts were normalised to that of *Gapdh*. (**D**) Schematic summary of biallelic transcription across the *H19* DMR and Ig-DMR in male germ cells at the time of imprint establishment. Transcripts are in the opposite direction of the main nearby genes, *H19* and *Gtl2*, respectively.

H19 DMR RNAs persisted at 17.5 d.p.c. (Figure 4A; Supplementary Figure S5), when almost full DNA methylation had been acquired (Figure 1). Similarly high levels were observed with primers pairs at the 5′ and the 3′ side of each of the ICRs (Figure 5A; Supplementary Figure S6). Sequencing of amplification products indicated that the germ cell transcripts at the Ig-DMR and *H19* DMR originated from both the parental chromosomes (Figure 4B). By analysing cDNA, reverse transcribed using stand-specific oligonucleotides, next we determined from which of the two DNA strands the male germ cell transcripts originated. At both the Ig-DMR and the *H19* DMR, transcription was detected from one strand predominantly. At the *H19* DMR, transcription originated predominantly from the side where the close-by *H19* gene is located. At the Ig-DMR, transcription was found to come from the side where the *Gtl2* gene is located (Figure 4C).

In further analyses, transcription was also detected between the *H19* DMR and the *H19* gene. With four primer pairs in the *H19* gene-upstream region A–D, comparably high transcript levels were detected, at both 15.5 and 17.5 d.p.c. (Figure 5A). Amplification of several longer RT–PCR fragments (Figure 5B) strongly suggests that these amplification events correspond to a single transcript, which is predominantly nuclear in its localisation (Supplementary Figure S7).

Importantly, no RT–PCR product was amplified in a region (region D–E, Figure 5B) overlapping the promoter of *H19* gene. Furthermore, at exon-1 of *H19* (region E) transcription was much higher than at the upstream regions A–D (Figure 5A), also suggesting that independent transcription events occur upstream and downstream of the *H19* promoter, respectively. Consistently, by strand-specific RT–PCR dedicated to amplify (*H19*) antisense transcription events, much higher levels of transcription were detected upstream (region D) than downstream (region E) of the *H19* promoter (Figure 5C). Combined, these data suggest that transcription across the *H19* DMR predominantly initiates upstream of the *H19* gene, which itself is highly transcribed in the male PGC cells as well. However, expression of the RNAs crossing the *H19* DMR seems not linked to the expression of the *H19* gene. In female PGCs, *H19* is more highly expressed than in male PGCs, whereas the antisense transcript crossing the *H19* DMR is expressed at highest levels in male PGCs. In somatic control cells, *H19* is expressed 25-fold higher than in the male PGCs, and yet, the upstream non-coding RNA (ncRNA) is not detected (Supplementary Figure S8).

Because of repeat sequences in this region, it was difficult to estimate the precise start site of the Ig-DMR transcripts in the male PGCs. However, transcription was detected at a region between the Ig-DMR and *Gtl2* as well, and cDNA amplification was readily achieved across this ICR (Supplementary Figure S6). Combined, our data indicate high levels of biallelic transcription across the Ig-DMR and *H19* DMR ICRs, on one of the two strands predominantly (Figure 5D). We assume that these are ncRNAs, given the absence of significant open reading frames (of >100 bp) in the regions concerned. The concordant levels of transcription across regions A–D for the *H19* DMR, and A-C the Ig-DMR (Figure 5A; Supplementary Figure S6) suggest that these ncRNAs are unspliced. Indeed, bio-informatic analysis (Genescan) shows that the *H19* and Ig-DMR and their flanking regions do not comprise canonical splice donor and acceptor sites.

Discussion

Our main finding is that maternal and paternal ICRs have distinct states of histone methylation and transcription at the time of imprint acquisition in male germ cells. At maternal ICRs, a strong correlation is found between promoter activity, H3 lysine-4 methylation and *in-vivo* protection against DNA methylation. Biallelic transcriptional read-through, and absence of H3K4me3, correlate with acquisition of DNA methylation at the paternal ICRs *H19* DMR and Ig-DMR. These data evoke the possibility that histone methylation

and transcriptional events are linked to the specificity of imprint acquisition in male germ cells.

Given the relatively high numbers of FACS-sorted cells that were still required, we focused our cChIP studies on histone modifications that could potentially influence DNA methylation. We found that maternal ICR promoters were biallelically active in male PGCs and this correlated with biallelic enrichment of H3K4me3, a mark which prevents recruitment of DNMT3A–DNMT3L complexes *in vitro* (Ooi *et al*, 2007; Zhang *et al*, 2010). We did not explore H3K4me2, since we failed to achieve allelic precipitation at ICRs in somatic control cells, indicating that the different sera tested were not good-enough for cChIP (Henckel *et al*, data not shown). Whether, similarly as in somatic cells (Mikkelsen *et al*, 2007; Zhao *et al*, 2007), all active promoters are marked by H3K4me3 in PGCs, is not known. However, high levels of H3K4me3 were detected at the control housekeeping genes and at the transcriptionally active *H19* gene as well. Gene promoters are generally active in male germ cells at the time of imprint acquisition (Guo *et al*, 2004). Indeed, at several other maternal ICRs (*Zac1, Grb10, Impact*), we detected promoter activity in the male germ cells as well (Supplementary Figure S4). Whether promoter-associated H3-lysine-4 methylation is maintained through post meiotic stages of spermatogenesis as well, is not known. However, at the KvDMR1 and *Snrpn* DMR, chromatin is enriched in H3K4me2/3 in post meiotic spermatocytes and elongating spermatids as well (Delaval *et al*, 2007).

In non-mammalian model species, including *Neurospora crassa* (Tamaru *et al*, 2003), H3K9me3 facilitates acquisition of DNA methylation. Our quantitative measurements following cChIP showed that by 13.5 d.p.c., this repressive mark was completely lost from ICRs in male (and female) germ cells. Although a recent ChIP study detected H3K9me3 at the *H19* DMR in male PGCs at this developmental stage, no quantitative data were included to assess its degree of enrichment (Lee *et al*, 2010). The complete depletion of H3K9me3 at ICRs observed in our study contrasts with the presence of H3K9me3 at pericentric chromatin, which does not decrease significantly during PGC development, at least till 13.5 d.p.c. (Seki *et al*, 2005). Also, at IAP elements we detected persistence of H3K9me3. At all ICRs analysed, we also noted depletion of H4K20me3 in the male (and female) PGCs. These repressive histone marks, therefore, do not signal subsequent acquisition of DNA methylation, at least not at the paternal ICRs.

The loss of H3K9me3 and H4K20me3 in PGCs complements our previous observation in mouse embryos that repressive histone modifications at ICRs depend on the presence of DNA methylation (Henckel *et al*, 2009). Consequently, the loss of H3K9me3 and H4K20me3 in PGCs could be linked to the active, wide-spread removal of DNA methylation which occurs from ~10 to 12.5 d.p.c. (Hajkova *et al*, 2002). Conversely, the deposition of these repressive marks onto the methylated alleles of ICRs most likely occurs after fertilisation only, in the developing embryo. In agreement with this scenario, the DNA methylation imprints at paternal ICRs are not associated with H3K9me3 and H4K20me3 in spermatocytes and spermatids (Delaval *et al*, 2007).

H2A/H4R3me2s was recently shown to be required for DNA methylation acquisition at the silenced *Globin* genes in primary erythroid progenitors, and this PRMT5-mediated H2A/H4 arginine methylation constituted a direct binding target of DNMT3A (Zhao *et al*, 2009). Since in early germ cells, BLIMP1 associates with PRMT5 to control global levels of H2A/H4R3me2s (Ancelin *et al*, 2006), we explored whether there could be enrichment of this mark at imprinted loci. Indeed, high levels of biallelic H2A/H4R3me2s were detected at ICRs in 13.5 and 15.5 d.p.c. germ cells. Although H2A/H4R3me2s has been hypothesised to facilitate DNMT3A recruitment at ICRs in male PGCs (Jelinic *et al*, 2006), it would not provide the signal indicating which ICRs need to become methylated since it was detected at both maternal and paternal ICRs.

In the male germ cells, we detected high levels of transcription through the *H19* DMR and Ig-DMR at 15.5 d.p.c., at the beginning of imprint establishment. Transcription levels were still high at 17.5 d.p.c., when methylation acquisition was almost complete. One hypothesis, therefore, could be that the acquired CpG methylation had led to enhanced transcription through these ICRs. A recent study on neurogenic gene loci provides evidence for such a mechanism in which DNA methylation enhances transcription (Wu *et al*, 2010). In an earlier study on post meiotic male germ cells (which have full DNA methylation at paternal ICRs), we did not detect transcription across the Ig-DMR and *H19*-DMR (Delaval *et al*, 2007). An alternative, non-exclusive, hypothesis is that transcription across the paternal ICRs facilitates imprint acquisition in the male PGCs. Insights into such a mechanism have recently been obtained relative to imprint acquisition in the female germ line. At the *Gnas* locus on mouse distal chromosome 2, DNA methylation acquisition in growing oocytes requires transcription across the ICR (Chotalia *et al*, 2009). How, precisely, transcription could contribute to acquisition of *de-novo* methylation in germ cells is unknown, but insights have emerged from studies on somatic cells. X-linked genes, for instance, have higher levels of DNA methylation on the transcriptionally active than on the inactive X chromosome (Hellman and Chess, 2007). The observed strand-preference of transcription across both *H19* DMR and Ig-DMR could be relevant in relation to recent work on rDNA genes, showing RNA-dependent acquisition of DNA methylation is linked to the formation of RNA–DNA triplexes (Schmitz *et al*, 2010). Together with insights from other model systems, our combined data make us to propose a working model (Figure 6) in which a specific histone modification state and transcriptional read-through, producing long ncRNAs, guide the acquisition of DNA methylation at paternal ICRs.

Imprinting acquisition in transgenic contexts has been observed for large constructs which comprised the ICR and sequences up to the 3′ part of the *H19* gene (Cranston *et al*, 2001). When ectopically inserted, the *H19* DMR itself is not sufficient for DNA methylation acquisition in male germ cells, although methylation can sometimes be acquired during early development (Matsuzaki *et al*, 2009). This finding agrees with a role of the observed transcriptional read-through initiating upstream of the *H19* gene in PGCs.

It seems unlikely that all paternal ICRs use the same imprinting mechanism. The *Rasgrf1* locus on mouse chromosome 9 is clearly different from the others, and was not included in this study. It does not have an equivalent in humans and its methylation acquisition requires not only

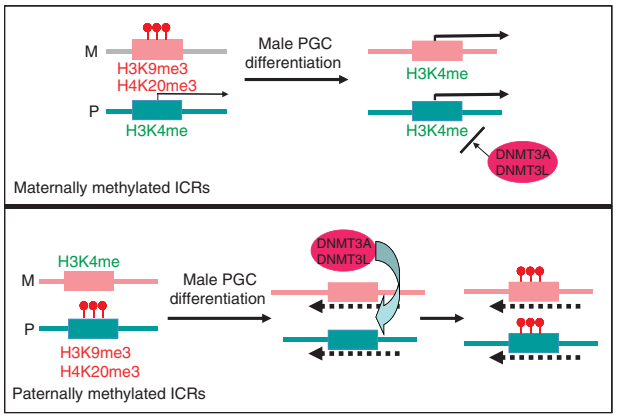

Figure 6 Model for imprint acquisition in male germ cells. At the maternally methylated ICRs (upper part), which comprise promoters, during male PGC differentiation there is loss of repressive histone methylation and acquisition of biallelic H3 K4 methylation. The latter correlates with biallelic promoter activity and prevents recruitment of DNMT3A–DNMT3L complexes to the DNA. At paternally methylated ICRs (lower part), there is also loss of allele-specific repressive histone methylation during male PGC differentiation, as well as a complete depletion of already-low levels of H3K4me3. Possibly involving facilitating histone modifications, such as H2A/H4R3me2s, this histone modification state allows recruitment of DNMT3A–DNMT3L complexes, the signal for which could be provided by transcription through these intergenic ICRs (dashed lines). Our data indicate that the model could be pertinent in particular for the Ig-DMR and the *H19* DMR.

DNMT3A, but also DNMT3B (Kato *et al*, 2007). Acquisition of the paternal imprint at this retrotransposed locus involves small RNAs and depends on the expression of Mili, Miwi2, and MitoPLD, all components of the PIWI-interacting RNA (piRNA) pathway (Shoji *et al*, 2009; Watanabe *et al*, 2011). Methylation at the *H19* DMR and Ig-DMR, in contrast, is not regulated by components of the piRNA pathway, and no small RNAs were detected in male germ cells at these ICRs (Shoji *et al*, 2009; Watanabe *et al*, 2006, 2011). Thus, whereas imprint acquisition at the Ig-DMR and *H19* DMR shows striking similarities to the mechanisms thought to control imprint establishment in oocytes (Chotalia *et al*, 2009; Ciccone *et al*, 2009), the process could be different at other paternal ICRs.

Materials and methods

Germ cell collection

Gonads were trypsinised in the presence of 0.2 mg/ml of DNAse-I, filtered through 40 μm cell strainers (BD Falcon™) and cells were sorted using a FACS-Aria™ (BD Biosciences). Both GFP-positive (germ cells) and GFP-negative (somatic control) cells were collected. On average, ~7000 germ cells were obtained per gonad.

Carrier ChIP

Drosophila melanogaster S2 cells were washed with PBS and mixed with mouse cells of interest (10 million S2 cells per 100 000 mouse cells). Nuclei were extracted as described (Umlauf *et al*, 2004; Henckel *et al*, 2009), resuspended in 200–300 μl of 'Nuclei PURE Storage Buffer' (SIGMA, S9183), and stored at −80°C. Batches of nuclei were thawed on ice and pooled to get ~75 000–100 000 mammalian cells of interest per ChIP. Chromatin was digested for 3 min at 37°C with MNase (at 7.5 U/ml, USB/Affymetrix), purified as described (Umlauf *et al*, 2004; Henckel *et al*, 2009), and precleared with 50 μl of protein-A sepharose overnight at 4°C before ChIP. Immunoprecipitations were performed in a 500-μl volume overnight at 4°C, with 10 μg of antibodies bound to Dynabeads protein-A magnetic beads (Invitrogen). Details on antibodies are in Supplementary Table S2. Bead-bound chromatin was washed with 1 ml of three successive washing buffers (Henckel *et al*, 2009), three times for each, and DNA was purified using NucleoSpin Extract II kit (Macherey Nagel). Primers used for qualitative and quantitative PCR analysis are provided in Supplementary Table S1. cChIP data were obtained from at least three (and up to five) assays, performed on independent chromatin preparations, except for the data on male germ cells at 15.5 d.p.c. (Figure 3A), which derived from two independent experiments.

Quantitative analysis of immunoprecipitated DNA by real-time PCR amplification

Input and antibody-bound fractions were quantified by real-time PCR amplification with a SYBR Green mixture (Qiagen) using an MX3000 apparatus (Stratagene). Background precipitation levels were determined by performing mock precipitations with a non-specific IgG antiserum (Sigma C-2288), and were only a fraction of that observed in the precipitations with specific antisera. Bound/Input ratios were calculated and were normalised, according to the antiserum used, against precipitation at IAP elements or *Rpl30*.

Bisulphite sequencing and RNA expression analysis

DNA extraction and bisulphite sequencing were conducted on batches of ~15 000 cells, as described (Henckel *et al*, 2009). For each region analysed, CpG methylation profiles were obtained from at least three independent bisulphite treatments, with analysis of two or more independent PCR products per treatment. For each amplicon, methylation patterns were also assessed by digestion with 'diagnostic' restriction endonucleases (the 'Cobra' approach) followed by direct sequencing (data not shown). The two different approaches gave concordant results.

For reverse transcription, total RNA was extracted from batches of 30 000–100 000 cells using Trizol Reagent (Invitrogen). After digestion with RNase-free DNase-I, first-strand cDNA was generated by reverse transcription with Superscript-II (Invitrogen), or Quantiteck Reverse transcript Kit (Qiagen), using randomised primers. Duplicate sets of control samples were produced with the reverse transcriptase omitted to detect amplification from contaminating DNA. PCR amplifications on the cDNAs were performed using gene-specific primers (Supplementary Table S1). RT–PCR products were quantified by real-time PCR amplification with a SYBR Green mix (Qiagen) using an MX3000 apparatus (Stratagene). *Gapdh* transcript levels were used for normalisation (Supplementary Table S1). RNA expression analyses were repeated at least three times (and up to six times).

Supplementary data

Supplementary data are available at *The EMBO Journal* Online (http://www.embojournal.org).

Acknowledgements

We thank Jérôme Cavaillé and Michael Weber for reading the manuscript; Azim Surani (Gurdon Institute, Cambridge, UK) and Wolf Reik (The Babraham Institute, Cambridge, UK) for the *Oct4*-GFP mice; and Myriam Boyer-Clavel and Cedric Mongellaz from the Montpellier RIO Imaging platform (MRI) for their help with cytometry. This work was grant supported by the Agence National de Recherche (ANR blanc 'EMPREINTE'), the European Chemical Industry Council (CEFIC) Long Research Initiative (EMSG49-CNRS-08), and La Ligue Contre le Cancer. AH acknowledges a PhD Fellowship received from the Association de Recherche contre le Cancer (ARC).
Author contributions: PA and RF designed the study; AH, PA, and SKK performed the experiments; KC supervised and organised the mouse embryology work; PA, RF and AH analysed the data; RF wrote the manuscript.

Conflict of interest

The authors declare that they have no conflict of interest.

References

Ancelin K, Lange UC, Hajkova P, Schneider R, Bannister AJ, Kouzarides T, Surani MA (2006) Blimp1 associates with Prmt5 and directs histone arginine methylation in mouse germ cells. *Nat Cell Biol* **8:** 623–630

Arnaud P (2010) Genomic imprinting in germ cells: imprints are under control. *Reproduction* **140:** 411–423

Bartolomei MS (2009) Genomic imprinting: employing and avoiding epigenetic processes. *Genes Dev* **23:** 2124–2133

Bernstein BE, Mikkelsen TS, Xie X, Kamal M, Huebert DJ, Cuff J, Fry B, Meissner A, Wernig M, Plath K, Jaenisch R, Wagschal A, Feil R, Schreiber SL, Lander ES (2006) A bivalent chromatin structure marks key developmental genes in embryonic stem cells. *Cell* **125:** 315–326

Bourc'his D, Xu GL, Lin CS, Bollman B, Bestor TH (2001) Dnmt3L and the establishment of maternal genomic imprints. *Science* **294:** 2536–2539

Chotalia M, Smallwood SA, Ruf N, Dawson C, Lucifero D, Frontera M, James K, Dean W, Kelsey G (2009) Transcription is required for establishment of germline methylation marks at imprinted genes. *Genes Dev* **23:** 105–117

Ciccone DN, Su H, Hevi S, Gay F, Lei H, Bajko J, Xu G, Li E, Chen T (2009) KDM1B is a histone H3K4 demethylase required to establish maternal genomic imprints. *Nature* **461:** 415–418

Cranston MJ, Spinka TL, Elson DA, Bartolomei MS (2001) Elucidation of the minimal sequence required to imprint H19 transgenes. *Genomics* **73:** 98–107

Davis TL, Yang GL, McCarrey JR, Bartolomei MS (2000) The H19 methylation imprint is erased and re-established differentially on the parental alleles during male germ cell development. *Hum Mol Genet* **9:** 2885–2894

Delaval K, Govin J, Cerqueira F, Rousseaux S, Khochbin S, Feil R (2007) Differential histone modifications mark mouse imprinting control regions during spermatogenesis. *EMBO J* **26:** 720–729

Drewell RA, Arney KL, Arima T, Barton SC, Brenton JD, Surani MA (2002) Novel conserved elements upstream of the H19 gene are transcribed and act as mesodermal enhancers. *Development* **129:** 1205–1213

Fitzpatrick GV, Soloway PD, Higgins MJ (2002) Regional loss of imprinting and growth deficiency in mice with a targeted deletion of KvDMR1. *Nat Genet* **32:** 426–431

Guo R, Yu Z, Guan J, Ge Y, Ma J, Li S, Wang S, Xue S, Han D (2004) Stage-specific and tissue-specific expression characteristics of differentially expressed genes during mouse spermatogenesis. *Mol Reprod Dev* **67:** 264–272

Hajkova P, Erhardt S, Lane N, Haaf T, El-Maarri O, Reik W, Walter J, Surani MA (2002) Epigenetic reprogramming in mouse primordial germ cells. *Mech Dev* **117:** 15–23

Hata K, Okano M, Lei H, Li E (2002) Dnmt3L cooperates with the Dnmt3 family of *de novo* DNA methyltransferases to establish maternal imprints in mice. *Development* **129:** 1983–1993

Hellman A, Chess A (2007) Gene body-specific methylation on the active X chromosome. *Science* **315:** 1141–1143

Henckel A, Nakabayashi K, Sanz LA, Feil R, Hata K, Arnaud P (2009) Histone methylation is mechanistically linked to DNA methylation at imprinting control regions in mammals. *Hum Mol Genet* **18:** 3375–3383

Hiura H, Sugawara A, Ogawa H, John RM, Miyauchi N, Miyanari Y, Horiike T, Li Y, Yaegashi N, Sasaki H, Kono T, Arima T (2010) A tripartite paternally methylated region within the Gpr1-Zdbf2 imprinted domain on mouse chromosome 1 identified by meDIP-on-chip. *Nucleic Acids Res* **38:** 4929–4945

Jelinic P, Stehle JC, Shaw P (2006) The testis-specific factor CTCFL cooperates with the protein methyltransferase PRMT7 in *H19* imprinting control region methylation. *PLoS Biol* **4:** e355

Kaneda M, Okano M, Hata K, Sado T, Tsujimoto N, Li E, Sasaki H (2004) Essential role for *de novo* DNA methyltransferase Dnmt3a in paternal and maternal imprinting. *Nature* **429:** 900–903

Kato Y, Kaneda M, Hata K, Kumaki K, Hisano M, Kohara Y, Okano M, Li E, Nozaki M, Sasaki H (2007) Role of the Dnmt3 family in *de novo* methylation of imprinted and repetitive sequences during male germ cell development in the mouse. *Hum Mol Genet* **16:** 2272–2280

Koide T, Moriwaki K, Uchida K, Mita A, Sagai T, Yonekawa H, Katoh H, Miyashita N, Tsuchiya K, Nielsen TJ, Shiroishi T (1998) A new inbred strain JF1 established from Japanese fancy mouse carrying the classic piebald allele. *Mamm Genome* **9:** 15–19

Lane N, Dean W, Erhardt S, Hajkova P, Surani A, Walter J, Reik W (2003) Resistance of IAPs to methylation reprogramming may provide a mechanism for epigenetic inheritance in the mouse. *Genesis* **35:** 88–93

Lee D-H, Singh P, Tsai SY, Oates N, Spalla A, Spalla C, Brown L, Rivas G, Larson G, Rauch TA, Pfeifer GP, Szabó PE (2010) CTCF-dependent chromatin bias constitutes transient epigenetic memory of the mother at the *H19-Igf2* imprinting control region in prospermatogonia. *PLOS Genet* **6:** e1001224

Li BZ, Huang Z, Cui QY, Song XH, Du L, Jeltsch A, Chen P, Li G, Li E, Xu GL (2011) Histone tails regulate DNA methylation by allosterically activating *de novo* methyltransferase. *Cell Res* **21:** 1172–1181

Lin SP, Youngson N, Takada S, Seitz H, Reik W, Paulsen M, Cavaille J, Ferguson-Smith AC (2003) Asymmetric regulation of imprinting on the maternal and paternal chromosomes at the Dlk1-Gtl2 imprinted cluster on mouse chromosome 12. *Nat Genet* **35:** 97–102

Matsuzaki H, Okamura E, Shimotsuma M, Fukamizu A, Tanimoto K (2009) A randomly integrated transgenic H19 imprinting control region acquires methylation imprinting independently of its establishment in germ cells. *Mol Cell Biol* **29:** 4595–4603

Mikkelsen TS, Ku M, Jaffe DB, Issac B, Lieberman E, Giannoukos G, Alvarez P, Brockman W, Kim TK, Koche RP, Lee W, Mendenhall E, O'Donovan A, Presser A, Russ C, Xie X, Meissner A, Wernig M, Jaenisch R, Nusbaum C *et al* (2007) Genome-wide maps of chromatin state in pluripotent and lineage-committed cells. *Nature* **448:** 553–560

O'Neill LP, VerMilyea MD, Turner BM (2006) Epigenetic characterization of the early embryo with a chromatin immunoprecipitation protocol applicable to small cell populations. *Nat Genet* **38:** 835–841

Ooi SK, Qiu C, Bernstein E, Li K, Jia D, Yang Z, Erdjument-Bromage H, Tempst P, Lin SP, Allis CD, Cheng X, Bestor TH (2007) DNMT3L connects unmethylated lysine 4 of histone H3 to *de novo* methylation of DNA. *Nature* **448:** 714–717

Otani J, Nankumo T, Arita K, Inamoto S, Ariyoshi M, Shirakawa M (2009) Structural basis for recognition of H4K4 methylation status by DNA methyltransferase 3A ATRX-DNMT3-DNMTL domain. *EMBO Rep* **10:** 1235–1241

Pannetier M, Julien E, Schotta G, Tardat M, Sardet C, Jenuwein T, Feil R (2008) PR-SET7 and SUV4-20H regulate H4 lysine-20 methylation at imprinting control regions in the mouse. *EMBO Rep* **9:** 998–1005

Schoenfelder S, Smits G, Fraser P, Reik W, Paro R (2007) Non-coding transcripts in the H19 imprinting control region mediate gene silencing in transgenic Drosophila. *EMBO Rep* **8:** 1068–1073

Schmitz KM, Mayer C, Postepska A, Grummt I (2010) Interaction of noncoding RNA with the rDNA promoter mediates recruitment of DNMT3b and silencing of rRNA genes. *Genes Dev* **24:** 2264–2269

Seki Y, Hayashi K, Itoh K, Mizugaki M, Saitou M, Matsui Y (2005) Extensive and orderly reprogramming of genome-wide chromatin modifications associated with specification and early development of germ cells in mice. *Dev Biol* **278:** 440–458

Shemer R, Birger Y, Riggs AD, Razin A (1997) Structure of the imprinted mouse Snrpn gene and establishment of its parental-specific methylation pattern. *Proc Natl Acad Sci USA* **94:** 10267–10272

Shoji M, Tanaka T, Hosokawa M, Reuter M, Stark A, Kato Y, Kondoh G, Okawa K, Chujo T, Suzuki T, Hata K, Martin SL, Noce T, Kuramochi-Miyagawa S, Nakano T, Sasaki H, Pillai RS, Nakatsuji N, Chuma S (2009) The TDRD9-MIWI2 complex is essential for piRNA-mediated retrotransposon silencing in the mouse male germline. *Dev Cell* **17:** 775–787

Tamaru H, Zhang X, McMillen D, Singh PB, Nakayama J, Grewal SI, Allis CD, Cheng X, Selker EU (2003) Trimethylated lysine 9 of histone H3 is a mark for DNA methylation in Neurospora crassa. *Nat Genet* **34:** 75–79

Tremblay KD, Saam JR, Ingram RS, Tilghman SM, Bartolomei MS (1995) A paternal-specific methylation imprint marks the alleles of the mouse H19 gene. *Nat Genet* **9:** 407–413

Umlauf D, Goto Y, Cao R, Cerqueira F, Wagschal A, Zhang Y, Feil R (2004) Imprinting along the Kcnq1 domain on mouse chromosome 7

involves repressive histone methylation and recruitment of Polycomb group complexes. *Nat Genet* **36:** 1296–1300

Verona RI, Thorvaldsen JT, Reese KJ, Bartolomei MS (2008) The transcriptional status but not the imprinting control region determines allele-specific histone modifications at the imprinted *H19* Locus. *Mol Cell Biol* **28:** 71–82

Watanabe T, Takeda A, Tsukiyama T, Mise K, Okuno T, Sasaki H, Minami N, Imai H (2006) Identification and characterization of two novel classes of small RNAs in the mouse germline: retrotransposon-derived siRNAs in oocytes and germline small RNAs in testes. *Genes Dev* **20:** 1732–1743

Watanabe T, Tomizawa S, Mitsuya K, Totoki Y, Yamamoto Y, Kuramochi-Miyagawa S, Iida N, Hoki Y, Murphy PJ, Toyoda A, Gotoh K, Hiura H, Arima T, Fujiyama A, Sado T, Shibata T, Nakano T, Lin H, Ichiyanagi K, Soloway PD *et al* (2011) Role of piRNA and non-coding RNA in *de novo* DNA methylation of the imprinted mouse *Rasgrf1* locus. *Science* **332:** 848–852

Wu H, Coskun V, Tao J, Xie W, Ge W, Yoshikawa K, Li E, Zhang Y, Sun YE (2010) Dnmt3a-dependent nonpromoter DNA methylation facilitates transcription of neurogenic genes. *Science* **329:** 444–448

Yoshimizu T, Sugiyama N, De Felice M, Yeom YI, Ohbo K, Masuko K, Obinata M, Abe K, Scholer HR, Matsui Y (1999) Germline-specific expression of the Oct-4/green fluorescent protein (GFP) transgene in mice. *Dev Growth Differ* **41:** 675–684

Zhang Y., Jurkowska R, Soeroes S, Rajavelu A, Dhayalan A, Bock I, Rathert P, Brandt O, Reinhardt R, Fischle W, Jeltsch A (2010) Chromatin methylation activity of Dnmt3a and Dnmt3a/3L is guided by interaction of the ADD domain with the histone H3 tail. *Nucleic Acids Res* **38:** 4246–4253

Zhao Q, Rank G, Tan YT, Li H, Moritz RL, Simpson RJ, Cerruti L, Curtis DJ, Patel DJ, Allis CD, Cunningham JM, Jane SM (2009) PRMT5-mediated methylation of histone H4R3 recruits DNMT3A, coupling histone and DNA methylation in gene silencing. *Nat Struct Mol Biol* **16:** 304–311

Zhao XD, Han X, Chew JL, Liu J, Chiu KP, Choo A, Orlov YL, Sung WK, Shahab A, Kuznetsov VA, Bourque G, Oh S, Ruan Y, Ng HH, Wei CL (2007) Whole-genome mapping of histone H3 Lys4 and 27 trimethylations reveals distinct genomic compartments in human embryonic stem cells. *Cell Stem Cell* **1:** 286–298